



X-ray induced demagnetization of single-molecule magnets

Jan Dreiser,^{1,2,a)} Rasmus Westerström,^{1,3,4} Cinthia Piamonteze,¹ Frithjof Nolting,¹ Stefano Rusponi,² Harald Brune,² Shangfeng Yang,⁵ Alexey Popov,⁶ Lothar Dunsch,⁶ and Thomas Greber^{3,b)}

¹Swiss Light Source, Paul Scherrer Institute, 5232 Villigen PSI, Switzerland

²Institute of Condensed Matter Physics, Ecole Polytechnique Fédérale de Lausanne, 1015 Lausanne, Switzerland

³Physik-Institut, Universität Zürich, 8057 Zürich, Switzerland

⁴Department of Physics and Astronomy, Uppsala University, 751 20 Uppsala, Sweden

⁵Hefei National Laboratory for Physical Sciences at Microscale, Department of Materials Science and Engineering, University of Science and Technology of China, 96 Jinzhai Road, Hefei 230026, China

⁶Department of Electrochemistry and Conducting Polymers, Leibniz Institute of Solid State and Materials Research, 01069 Dresden, Germany

(Received 27 May 2014; accepted 16 July 2014; published online 25 July 2014)

Low-temperature x-ray magnetic circular dichroism measurements on the endohedral single-molecule magnet DySc₂N@C₈₀ at the Dy M_{4,5} edges reveal a shrinking of the opening of the observed hysteresis with increasing x-ray flux. Time-dependent measurements show that the exposure of the molecules to x-rays resonant with the Dy M₅ edge accelerates the relaxation of magnetization more than off-resonant x-rays. The results cannot be explained by a homogeneous temperature rise due to x-ray absorption. Moreover, the observed large demagnetization cross sections indicate that the resonant absorption of one x-ray photon induces the demagnetization of many molecules. © 2014 AIP Publishing LLC. [<http://dx.doi.org/10.1063/1.4891485>]

Single-molecule magnets (SMMs)^{1–5} have attracted a lot of interest in view of possible applications in molecular spintronics,^{6,7} and quantum information processing schemes.⁸ SMMs are formed by one or more magnetic ions surrounded by ligands which induce magnetic anisotropy. The anisotropy in turn leads to a blocking of the magnetization. If the resulting magnetization relaxation times are long enough they are manifested by the opening of a magnetic hysteresis. There is growing interest in x-ray magnetic circular dichroism (XMCD) to study SMMs because of its ability to detect element-resolved magnetic moments combined with submonolayer sensitivity.^{9–14}

XMCD has been used to observe magnetic hysteresis, i.e., nonequilibrium magnetization in SMMs.^{11–13} Here, we demonstrate that in endohedral SMMs the x-ray exposure itself can lead to an acceleration of magnetization relaxation. The x-ray induced demagnetization can be understood by the creation of small volumes of excited, or hot, molecules by the secondary electrons emitted from the Auger decay of the x-ray induced core hole. In this study, we use the single ion member of the lanthanide based endohedral SMM family¹⁵ DySc₂N@C₈₀.¹⁶ It is the simplest member with very weak intermolecular coupling. It exhibits magnetization relaxation times of several hours at $T = 2$ K in a small applied magnetic field and no measurable *chemical* degradation, e.g., due to bond breaking by x-rays or because of x-ray induced desorption of the magnetic species.¹⁷ Our results explain why often superconducting interference device (SQUID) and XMCD measurements qualitatively give the same result, but they differ when a precise quantitative comparison is done, e.g., the observation of smaller hysteresis openings in XMCD.

The findings are thus of relevance for all experiments investigating SMMs by XMCD, showing that obtained values for relaxation times might be too small.

Samples were prepared by drop casting DySc₂N@C₈₀ dissolved in toluene onto aluminum plates until a black residue was clearly visible by eye. X-ray absorption spectroscopy (XAS) was performed at the X-Treme beamline¹⁸ at the Swiss Light Source, Paul Scherrer Institute with a cold finger temperature of 2 K and at magnetic fields of up to 7 T. All measurements were done using a defocused x-ray spot of $\sim 1 \times 1$ mm². The x-ray flux was measured with a 10×10 mm² Si photodiode (AXUV100 from Intl. Radiation Detectors Inc.) located after the last optical element of the beam line. The x-ray spot size was determined by moving horizontally and vertically sharp blades through the beam. Detailed information about the employed metal nitride cluster endofullerenes can be found elsewhere.^{19,20}

The XAS and XMCD of DySc₂N@C₈₀ obtained in total electron yield (TEY) mode at the Dy M_{4,5} edges are plotted in Fig. 1. The M₅ edge exhibits the characteristic triple peak structure determined by the selection rules $\Delta J = 0, \pm 1$ for electric dipole transitions, and in the XMCD the strongest features of both M₄ and M₅ edges are pointing upwards indicating a significant orbital angular momentum in line with the ⁶H_{15/2} ground state multiplet predicted by Hund's rules. From sum rules spin and orbital angular momentum values, $\langle S_z \rangle = 1.2(1)$ and $\langle L_z \rangle = 1.9(2)$ are obtained assuming $n_h = 5$ holes in the *f* shell. These values are lower by a factor of ~ 2 compared to the free Dy^{III} ion because of strong magnetic anisotropy and the random orientation of the molecules in the sample. The ratio between both angular momentum values can be derived without assumptions on the number of *f* holes. It evaluates to $\langle L_z \rangle / \langle S_z \rangle = 1.6(3)$ and is lower than expected from Hund's rules consistent with what was found previously.¹⁶

^{a)}Electronic mail: jan.dreiser@epfl.ch

^{b)}Electronic mail: greber@physik.uzh.ch

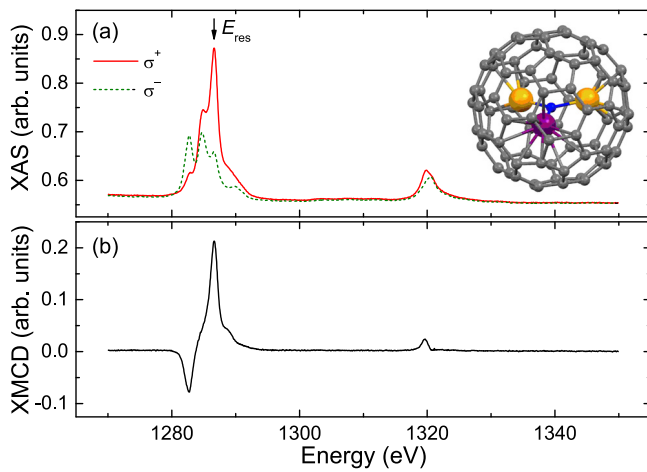


FIG. 1. Example (a) XAS and (b) XMCD spectra obtained on a drop cast sample of DySc₂N@C₈₀ at the Dy M_{4,5} edges with a cold finger temperature of 2 K and at $\mu_0 H = -6.0$ T. The structure of the molecule is shown as an inset with the Dy atom of the endohedral unit pointing towards the reader.

Hysteresis curves obtained by XMCD on DySc₂N@C₈₀ for varying x-ray fluxes are shown in Fig. 2. Clearly, increasing the flux leads to a smaller opening of the hystereses. We have verified that irreversible radiation damage, i.e., chemical degradation, is absent by first increasing and then lowering the flux which revealed the shrinking and re-expansion of the hysteresis. To investigate further the magnitude and origin of the x-ray induced closing of the hysteresis, time-dependent relaxation measurements towards the corresponding equilibrium magnetization were performed. The field was ramped up to $\mu_0 H = 6.5$ T and then lowered to 0.2 T at a speed of 2 T/min. After reaching 0.2 T, the XMCD was measured using an alternating on-off resonance scheme, i.e., the x-rays were always illuminating the sample but their energy was changed within intervals of $\Delta t_{\text{tot}} = 20$ s, with the on resonance ratio $\kappa = \Delta t_{\text{on}}/\Delta t_{\text{tot}}$ being the parameter that allows the extraction of the influence of resonant absorption. The same sequence with a given κ was repeated twice for both circular polarizations of the x-rays. Further, several

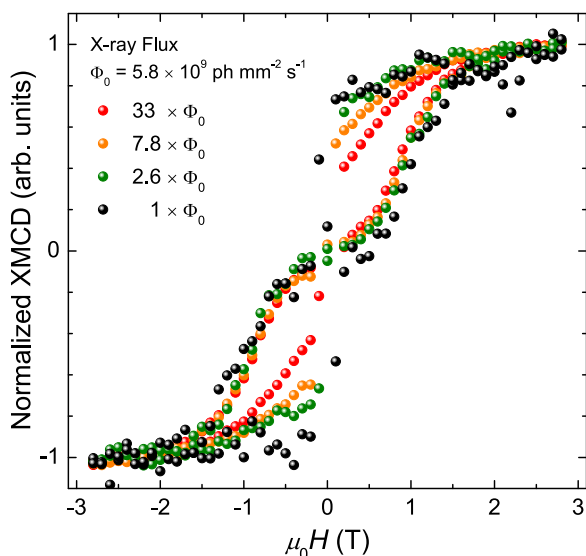


FIG. 2. Flux-dependent hysteresis curves obtained on DySc₂N@C₈₀ by XMCD with a cold finger temperature of 2 K. Field scan rate: 2 T/min.

measurements were carried out with varying κ . Two representative XMCD decay curves with $\kappa_1 = 9.1\%$ and $\kappa_2 = 91\%$ are shown in Fig. 3 revealing a larger relaxation rate at resonance. Solid lines represent single-exponential fits demonstrating that the magnetization relaxation proceeds with a characteristic time τ .

The observed relaxation rates $\Gamma_{\text{exp}} = \tau^{-1}$ extracted from exponential fits to the time-dependent measurements on DySc₂N@C₈₀ for varying ratios κ and two different x-ray fluxes Φ are plotted in Fig. 4(a). Obviously, increasing the fraction of time when x-rays are on resonance with the Dy M₅ edge leads to an increase of the relaxation rate. Furthermore, the relaxation rate increases with x-ray flux. Extrapolated values for $\kappa = 0\%$ and 100% are plotted in Fig. 4(b) showing that both rates are increasing with the x-ray flux. The increase is more pronounced for the resonant case and the data in Fig. 4(b) indicate an intrinsic relaxation rate of 0.5 min⁻¹ at zero flux consistently found for both resonant and nonresonant cases. Indeed, the resonant and nonresonant rates should coincide at the zero-flux point since in this condition the x-ray energy is irrelevant. The translation of this relaxation rate to a temperature using the Arrhenius law $\tau_{\text{Arrh}} = \tau_0 \exp[\Delta E_{\text{eff}}/(k_B T)]$ with the parameters of Ref. 16 results in an effective temperature in the absence of x-rays of approximately 5 K. The quantum tunneling of magnetization was neglected because it is only relevant at smaller rates and lower temperatures.

In the following, we will show that the magnitude of the demagnetization effect cannot be reconciled with a homogeneous warming of the sample or its topmost layers by the x-rays. At a given flux, the heat input per unit area is constant since the soft x-rays used here are fully absorbed in the sample independent of their exact energy. In consequence, this rules out any explanation of the observed demagnetization effect by a homogeneous and depth-independent warming of the sample. When assuming a depth-dependent temperature distribution along the surface normal $T = f(z)$, originating from, e.g., a weak thermal coupling of the sample top layer, heat deposited by the x-rays distributes differently in the sample for on and off resonance according to the absorption

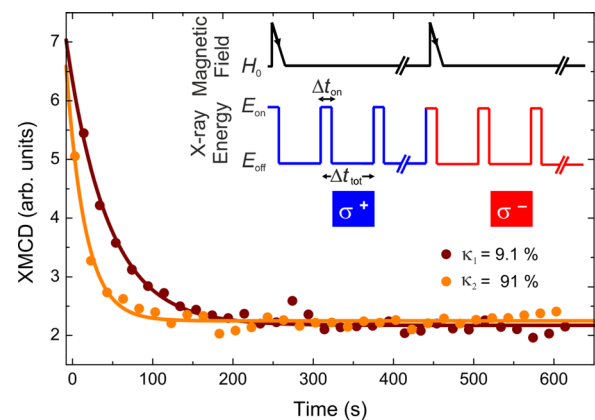


FIG. 3. Time-dependent XMCD curves obtained on DySc₂N@C₈₀ for different ratios of on-resonance vs. total x-ray exposure times $\kappa = \Delta t_{\text{on}}/\Delta t_{\text{tot}}$. The timing scheme is shown in the inset. $E_{\text{on}} = 1285.4$ eV and $E_{\text{off}} = 1250.0$ eV. At $t = 0$, the magnetic field reached its final value of $\mu_0 H_0 = 0.2$ T. The cold finger temperature was set to 2 K and the x-ray flux was $\Phi = 1.9 \times 10^{11}$ ph mm⁻² s⁻¹.

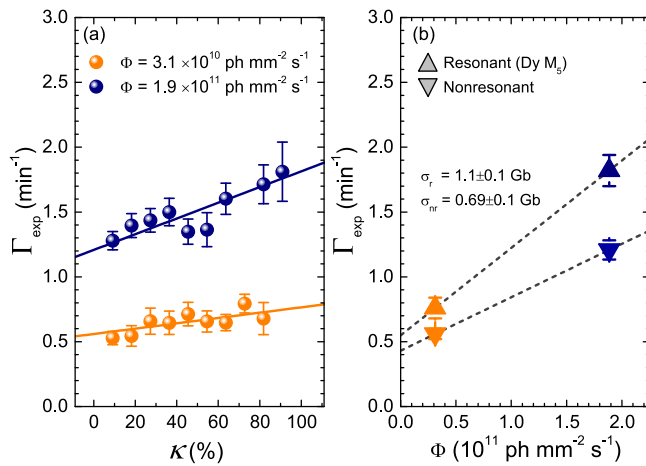


FIG. 4. (a) Experimentally determined relaxation rates Γ_{exp} of DySc₂N@C₈₀ for two different fluxes as a function of $\kappa = \Delta t_{\text{on}}/\Delta t_{\text{tot}}$ and (b) flux dependence of Γ_{exp} for $\kappa=0\%$ and $\kappa=100\%$. The extrapolation to zero flux allows to determine an effective temperature by comparing with SQUID data.¹⁶

strength. If the heating due to the x-rays is proportional to the corresponding total electron yield Y , which is taken as the average between left and right hand circularly polarized light, we obtain with the M_5 peak-to-background ratio Y (κ_2): $Y(\kappa_1) = 1.13$, i.e., a 13% higher heating rate on resonance as compared to off resonance. Indeed, this compares to the same value of a 13% higher effective temperature of 6.9 K (κ_2) vs. 6.1 K (κ_1) obtained from the translation of the relaxation rates to temperatures described beforehand using the Arrhenius law. This suggests that the effective temperature is proportional to the TEY, yielding an upper bound for a homogeneous temperature rise of the sample top layer due to the x-rays of 2 K. This bound is still compatible with the $T=f(z)$ type temperature distribution. In contrast, when the magnetization as measured with XMCD is used as a local thermometer, a significantly smaller upper bound is obtained: The equilibrium XMCD, i.e., the XMCD in the limit of $t \rightarrow \infty$ is proportional to the equilibrium magnetization in the applied field of 0.2 T. The equilibrium magnetization must decrease if the temperature increases. From this, we can state with the equilibrium data in Fig. 3 that $T_{\infty}(\kappa_1)$ is within a confidence interval of 80% not more than 2% lower than $T_{\infty}(\kappa_2)$. This finding is absolutely inconsistent with the temperature difference between 6.9 K (κ_2) and 6.1 K (κ_1) mentioned before, corroborating that these temperatures are only effective temperatures.

Given these considerations the constraint of a solely depth-dependent temperature profile $T=f(z)$ needs to be relaxed. Because the observed changes of the magnetization relaxation rate are not related to a laterally homogeneous, depth dependent temperature increase, it is justified to employ effective demagnetization cross sections for the x-ray induced processes. We proceed by evaluating the on and off resonant cross sections, and by proposing a model with local heating $T=f(x, y, z, t)$ due to the energy dissipation of the photo excitation.

The total magnetization relaxation rate is given by the sum of the rates of the individual relaxation processes $\Gamma_{\text{exp}} = \Gamma_x(\omega, \Phi) + \Gamma_i(T, H)$, where the first term refers to

the x-ray induced processes with $E_{\text{ph}} = \hbar\omega$ the energy of the x-ray photons and Φ the x-ray flux. The second term gives the temperature and magnetic-field dependent intrinsic relaxation rate that the molecules exhibit in the absence of the x-ray illumination. The data furthermore allow for the extraction of the demagnetization cross sections for off- and on-resonant photons. Accordingly, the cross-sections σ for the on- and off-resonant cases can be extracted using

$$\Gamma_x(\omega, \Phi) = \sigma(\omega) \times \Phi, \quad (1)$$

hence the cross sections of the resonant and non-resonant processes σ_r and σ_{nr} , respectively, can be determined from the data. We obtain $\sigma_r = 1.1 \pm 0.1 \text{ Gb/molecule}$ with $1 \text{ b} = 10^{-24} \text{ cm}^{-2}$ and $\sigma_{nr} = 0.69 \pm 0.1 \text{ Gb/molecule}$. Because of the presence of an energy-independent background the cross section $\sigma_{3d \rightarrow 4f}$ due to the resonant Dy $3d \rightarrow 4f$ excitations is likely to be even larger. These cross sections are extremely large compared to those for the excitation of an electron into the continuum which are less than a few Mb/atom for all elements contained in the investigated samples, as estimated from tabulated values. The so-called white line cross section which corresponds to local atomic-like excitations of Dy^{III} from the $3d^{10}4f^0$ ground state to the $3d^94f^{10}$ final states²¹ is, of course, largest ($\sigma_{\text{WL}} = 25 \text{ Mb/atom}$ at the M_5 edge for Dy metal²²) but still orders of magnitude smaller than the observed cross sections. Resonant excitation appears to be more efficient for demagnetization than non-resonant excitation. One reason for this is the different x-ray attenuation length, on and off resonance, respectively. In the following, we give a possible explanation for $\sigma_{3d \rightarrow 4f}$ on the basis of local excitations due to the deposited photon energy of approximately 1.3 keV. The ratio between $\sigma_{3d \rightarrow 4f}$ and σ_{WL} indicates that one resonant excitation at the Dy M_5 edge relaxes more than 50 molecules. The photon energy is dissipated to the sample *via* the Auger electron ($\sim 99\%$ probability) emitted upon the decay of the Dy core hole created by the absorption of a single x-ray photon. Fluorescence decay ($\sim 1\%$ probability) is negligible here. This Auger electron is scattered inelastically and converts its energy locally into heat. The resulting heat bump, initially localized in a small volume determined by the scattering length of the Auger electron and the resulting secondary electrons, is proposed to be responsible for the magnetization relaxation of the molecules. The energy is dissipated along the trajectories of the secondary electrons, likely in packets of plasmonic excitations.^{23,24} Mechanisms such as reversible structural changes leading to a faster quantum tunneling, i.e., relaxation of magnetization cannot be resolved, because the efficiency for such a process would be the demagnetization of one molecule per photon, in contrast to the observed efficiency of ~ 50 molecules per photon.

In order to demonstrate the plausibility of magnetization relaxation by heat bumps, we assume a temperature increase from 0 to 20 K which would be realized for 4×10^5 C₆₀ molecules given the absorption of a 1.3 keV photon.²⁵ At 20 K, the extrapolated magnetization decay time of DySc₂@C₈₀ is 3 s,¹⁶ i.e., 100 out of the 4×10^5 molecules reverse their magnetic moment in 2 ms. It cannot be excluded that faster mechanisms exist which allow for a transfer of the photo-

excitation to the magnetic moment of the endohedral unit before the relatively slow thermalization via phonons. The exact determination of the energy transfer cascade from Auger or secondary electrons to the magnetized molecules is beyond the scope of this work. Of course, the estimations presented beforehand are coarse, yet they support the idea that local thermal bumps due to the dissipation of the x-ray photon energy typically demagnetize 50 molecules, and that this energy is dissipated to the heat bath of the sample before a second photon hits the site, i.e., faster than in 25 s. As long as the heat conductivity, the x-ray absorption cross sections and fluxes are similar to the present system, x-ray induced heat bumps will not lead to a large increase in temperature at macroscopic length scales. Therefore, low temperature studies with x-rays are reasonable, if the flux is low, or if the x-ray pulse is shorter than, e.g., the characteristic spin flip times.

The reason why the x-ray induced heat bumps are more effective in the demagnetization of the SMMs, as compared to the case in which x-rays would heat homogeneously the whole sample or its top layers, can be found in the superlinear, in case of Arrhenius-type excitations exponential, increase of the SMM magnetization relaxation rate with temperature: In the case of a spatially homogenous weak temperature increase less molecules are relaxed than for the inhomogeneous scenario in which locally a rather large temperature increase occurs. Our results complement recent findings of demagnetization effects triggered by visible light.²⁶ In this reference, it was suggested that XMCD measurements could preclude the efficient detection of SMMs since the high-energy photon irradiation greatly disturbs the spin state or magnetization of the illuminated molecules. Here, we find that SMM hystereses can look slightly different under x-ray exposure as compared to methods in the dark (e.g., SQUID) for the case of DySc₂N@C₈₀. Furthermore, we quantify the cross section for the demagnetization processes which is orders of magnitude larger than that for the demagnetization of a single molecule by one resonant x-ray photon. These cross sections are obtained for densely packed DySc₂N@C₈₀ samples, and it is expected to decrease if the magnetic center density is decreased.

In conclusion, it is clearly possible to detect hystereses with XMCD, even at the largest x-ray fluxes. Nevertheless, time and flux dependent XMCD measurements show that x-rays can lead to an increased magnetization relaxation rate of SMMs. This is seen in systematic time-dependent experiments where the x-rays are probing the SMMs only for a given fraction of time on the M₅ resonance but otherwise they are detuned in energy. The results suggest that the x-ray induced demagnetization of SMMs depends on the x-ray dose. Our simple model based on local heating predicts that our results apply to all hysteresis and relaxation studies of SMMs using XMCD, which is the technique of choice for dilute or ultrathin magnetic systems such as SMMs deposited on surfaces, or when element specificity is needed.

The x-ray absorption measurements were performed on the EPFL/PSI X-Treme beamline at the Swiss Light Source,

Paul Scherrer Institute, Villigen, Switzerland. We acknowledge financial support from the Swiss National Science Foundation (R'Equip program, Proposal No. 206021-117410 and Ambizione program (J.D.), Grant No. PZ00P2_142474) and from the EPFL. R.W. acknowledges funding by the Swedish research council (350-2012-295). Further, we acknowledge funding by the Deutsche Forschungsgemeinschaft (Projects PO 1602/1-1 to A.A.P. and DU225/31-1 within the D-A-CH program).

- ¹R. Sessoli, D. Gatteschi, A. Caneschi, and M. A. Novak, *Nature* **365**, 141 (1993).
- ²J. R. Friedman, M. P. Sarachik, J. Tejada, and R. Ziolo, *Phys. Rev. Lett.* **76**, 3830 (1996).
- ³G. Christou, D. Gatteschi, D. N. Hendrickson, and R. Sessoli, *MRS Bull.* **25**, 66 (2000).
- ⁴R. Winpenny, *Single-Molecule Magnets and Related Phenomena* (Springer, Berlin, 2006).
- ⁵D. Gatteschi, R. Sessoli, and J. Villain, *Molecular Nanomagnets* (Oxford University Press, 2006).
- ⁶A. R. Rocha, V. M. Garcia-Suarez, S. W. Bailey, C. J. Lambert, J. Ferrer, and S. Sanvito, *Nat. Mater.* **4**, 335 (2005).
- ⁷L. Bogani and W. Wernsdorfer, *Nat. Mater.* **7**, 179 (2008).
- ⁸M. N. Leuenberger and D. Loss, *Nature* **410**, 789 (2001).
- ⁹P. Gambardella, S. Rusponi, M. Veronese, S. S. Dhesi, C. Grazioli, A. Dallmeyer, I. Cabria, R. Zeller, P. H. Dederichs, K. Kern, C. Carbone, and H. Brune, *Science* **300**, 1130 (2003).
- ¹⁰M. Mannini, P. Sainctavit, R. Sessoli, C. CartierditMoulin, F. Pineider, M.-A. Arrio, A. Cornia, and D. Gatteschi, *Chem. Eur. J.* **14**, 7530 (2008).
- ¹¹M. Mannini, F. Pineider, P. Sainctavit, C. Danieli, E. Otero, C. Sciancalepore, A. M. Talarico, M.-A. Arrio, A. Cornia, D. Gatteschi, and R. Sessoli, *Nat. Mater.* **8**, 194 (2009).
- ¹²L. Margheriti, D. Chiappe, M. Mannini, P. Car, P. Sainctavit, M.-A. Arrio, F. B. de Mongeot, J. C. Cezar, F. M. Piras, A. Magnani, E. Otero, A. Caneschi, and R. Sessoli, *Adv. Mater.* **22**, 5488 (2010).
- ¹³M. Gondec, R. Biagi, V. Corradini, F. Moro, V. De Renzi, U. del Pennino, D. Summa, L. Muccioli, C. Zannoni, D. B. Amabilino, and J. Veciana, *J. Am. Chem. Soc.* **133**, 6603 (2011).
- ¹⁴G. van der Laan and A. I. Figueroa, *Coord. Chem. Rev.* (published online).
- ¹⁵R. Westerström, J. Dreiser, C. Piamonteze, M. Muntwiler, K. Krämer, S.-X. Liu, S. Decurtins, A. Popov, S. Yang, L. Dunsch, and T. Greber, *Phys. Rev. B* **89**, 060406 (2014).
- ¹⁶R. Westerström, J. Dreiser, C. Piamonteze, M. Muntwiler, S. Weyeneth, H. Brune, S. Rusponi, F. Nolting, A. Popov, S. Yang, L. Dunsch, and T. Greber, *J. Am. Chem. Soc.* **134**, 9840 (2012).
- ¹⁷A. Lehnert, S. Rusponi, M. Etzkorn, S. Ouazi, P. Thakur, and H. Brune, *Phys. Rev. B* **81**, 104430 (2010).
- ¹⁸C. Piamonteze, U. Flechsig, S. Rusponi, J. Dreiser, J. Heidler, M. Schmidt, R. Wetter, M. Calvi, T. Schmidt, H. Pruchova, J. Krempasky, C. Quitmann, H. Brune, and F. Nolting, *J. Synchrotron Radiat.* **19**, 661 (2012).
- ¹⁹S. Stevenson, G. Rice, T. Glass, K. Harich, F. Cromer, M. R. Jordan, J. Craft, E. Hadju, R. Bible, M. M. Olmstead, K. Maitra, A. J. Fisher, A. L. Balch, and H. C. Dorn, *Nature* **401**, 55 (1999).
- ²⁰S. Yang, A. A. Popov, C. Chen, and L. Dunsch, *J. Phys. Chem. C* **113**, 7616 (2009).
- ²¹B. T. Thole, G. van der Laan, J. C. Fuggle, G. A. Sawatzky, R. C. Karnatak, and J.-M. Esteva, *Phys. Rev. B* **32**, 5107 (1985).
- ²²F. C. Vicentin, S. Turchini, F. Yubero, J. Vogel, and M. Sacchi, *J. Electron Spectrosc. Relat. Phenom.* **74**, 187 (1995).
- ²³A. Lucas, G. Gensterblum, J. J. Pireaux, P. A. Thiry, R. Caudano, J. P. Vigneron, P. Lambin, and W. Krätschmer, *Phys. Rev. B* **45**, 13694 (1992).
- ²⁴E. Sohmen, J. Fink, and W. Krätschmer, *Z. Phys. B: Condens. Matter* **86**, 87 (1992).
- ²⁵W. P. Beyermann, M. F. Hundley, J. D. Thompson, F. N. Diederich, and G. Grüner, *Phys. Rev. Lett.* **68**, 2046 (1992).
- ²⁶B. Donnio, E. Rivière, E. Terazzi, E. Voirin, C. Aronica, G. Chastanet, D. Luneau, G. Rogez, F. Scheurer, L. Joly, J.-P. Kappler, and J.-L. Gallani, *Solid State Sci.* **12**, 1307 (2010).